Applied Catalysis B: Environmental 94 (2010) 77–84

Contents lists available at ScienceDirect

Applied Catalysis B: Environmental

journal homepage: www.elsevier.com/locate/apcatb

Elucidation of structure–activity relationships of model three way catalysts for the combustion of methane

M. Santhosh Kumar [a,*], A. Eyssler [a], P. Hug [a], N. van Vegten [b], A. Baiker [b], A. Weidenkaff [a], D. Ferri [a,*]

[a] Empa, Laboratory for Solid State Chemistry and Catalysis, Ueberlandstrasse 129, CH-8600 Dübendorf, Switzerland
[b] Institute of Chemical and Bioengineering, ETH Zurich, Wolfgang – Pauli – Strasse 10, CH-8093, Zurich, Switzerland

ARTICLE INFO

Article history:
Received 25 August 2009
Received in revised form 19 October 2009
Accepted 23 October 2009
Available online 5 November 2009

Keywords:
Methane combustion
Model three way catalysts
$Pd/CeZrO_2$
$Pd/LaFeO_3$
In situ XANES
Active sites

ABSTRACT

The combustion of methane on model three way catalysts (TWC) $Pd/CeZrO_2$ and $Pd/LaFeO_3$ (2 wt.% Pd) was studied under lean conditions in the temperature range between ca. 200 and 800 °C to investigate the catalytic performance at and after high temperatures. The catalysts were prepared by incipient wetness impregnation and the nature and distribution of palladium species was characterized by N_2-physisorption, X-ray diffraction (XRD), visible Raman spectroscopy, X-ray absorption spectroscopy (XANES and EXAFS), H_2-temperature programmed reduction (H_2-TPR), CO adsorption followed by diffuse reflectance infrared Fourier transform spectroscopy (CO-DRIFTS) and CO chemisorption. The behaviour of Pd during the combustion was monitored by in situ XANES spectroscopy. The characterization results indicate that the dispersion of Pd is higher in $Pd/CeZrO_2$ than in $Pd/LaFeO_3$. The catalytic data reveal that $Pd/CeZrO_2$ is more active and stable compared to $Pd/LaFeO_3$ in the whole studied temperature range. This is also true even after subjecting the catalysts to reaction at $\geq$800 °C as evidenced by the extent of hysteresis observed in the conversion profiles. In situ XANES studies indicate that palladium had been in the oxidized state when the catalysts showed the best combustion performance. The studies also indicate that a fraction of PdO_x had been reduced when the hysteresis was observed in the conversion profiles (while cooling between ca. 680 and 560 °C) implying that the PdO_x species are the active sites, at least at $T \leq 700$ °C.

1. Introduction

Catalytic combustion of methane is an important topic in environmental catalysis due to its acute global warming potential, which is 21 times higher than that of CO_2 [1]. Therefore, combustion of methane to CO_2 and H_2O in a wide temperature range is of interest to treat exhaust of natural gas (CNG) fuelled vehicles, for example cars [2–7]. The latest technology to treat automotive exhaust gas is based on either $Pd/CeZrO_2$ catalysts or Pd-based perovskites (e.g., $LaFe_{0.95}Pd_{0.05}O_3$ based catalysts) [5,8–14]. Three way catalysts (TWC), undoubtedly, are the most effective in the abatement of nitrogen oxides (NO_x), CO and unburned hydrocarbons from the exhaust of the gasoline fuelled vehicles that comply with the present day emission regulations [8]. However when TWC are adapted to natural gas powered vehicles, their catalytic performance deteriorates relatively fast and methane emission becomes alarmingly high. Thus, improving the catalyst combustion activity and durability is the subject of intense ongoing research [3,12,15,16].

So far studies on combustion of methane dealt mostly with Pd/Al_2O_3 and Pd/ZrO_2 [17–24]. Some of these studies which report the catalytic performance in a wide temperature range (ca. 200–900 °C) show a loss in the combustion activity typically in the temperatures between 550 and 700 °C, especially after experiencing high temperatures (e.g., $T > 700$ °C). From thermal analysis (e.g., TGA) it was found that PdO decomposes into metallic Pd at certain temperatures depending on the nature of the catalyst and O_2 partial pressure [11–13,17,19,25]. The temperature was correlated with that of the hysteresis and PdO_x species were suggested as the active sites. Nevertheless, the nature of active palladium (here after referred as Pd) species for the combustion of methane is still a subject of debate. The combustion activity is attributed to a variety of Pd species, for example metallic Pd [20], PdO [17,19,22], thin layer of PdO on metallic Pd [21,26] and mixed Pd^0/PdO_x phase [27]. However, with respect to the model three-way $Pd/CeZrO_2$ catalysts very few studies on the combustion of methane are reported. These are limited to low temperatures ($T < 600$ °C) where a complete conversion of methane was observed [5,28,29]. Studies on the catalytic behaviour of Pd/

* Corresponding authors. Tel.: +41 44 823 4762; fax: +41 44 823 4041.
E-mail addresses: santhosh.matam@empa.ch (M. Santhosh Kumar), davide.ferri@empa.ch (D. Ferri).

0926-3373/$ – see front matter © 2009 Elsevier B.V. All rights reserved.
doi:10.1016/j.apcatb.2009.10.023

$CeZrO_2$ at high temperatures (after exposure to temperatures well above 700 °C, which often occurs in the catalytic converters) are largely missing.

With regard to Pd-based perovskites most of the studies are limited to reduction of NO (including SCR of NO with H_2), CO oxidation, behaviour of Pd under redox (typically reduced with H_2 and oxidized with O_2) conditions and total hydrocarbon (other than methane and represent gasoline fuel) conversion [8–10,14]. However, recent studies on the $Pd/LaMnO_x$ based perovskites at temperatures between 300 and 800 °C show, in general, poor activity especially in the temperature range where hysteresis was observed [12,13]. It is noteworthy that this is a typical operating temperature range of a catalytic converter in a vehicle [3].

Against this background, the objectives of this work are to assess (i) the performance of model three-way $Pd/CeZrO_2$ and $Pd/LaFeO_3$ catalysts (≈2 wt.% Pd) in the combustion of methane under lean conditions in a wide temperature range (between ca. 200 and 850 °C) that represent real operation of an automobile (especially after high temperatures), and (ii) the behaviour of Pd species during the reaction (i.e., elucidation of the structure and activity relationships). To this end, the catalysts were characterized by a variety of physico-chemical techniques to assess the nature and distribution of Pd species and their performance in the combustion of methane was studied in a fixed bed reactor. The behaviour of Pd species in the catalysts during the combustion of methane was monitored by X-ray absorption near edge structure (XANES). The results suggest that Pd is highly dispersed on both supports, $CeZrO_2$ and $LaFeO_3$, the dispersion being the highest on the former which exhibits superior combustion performance compared to the latter in the whole temperature range studied. In situ XANES evidenced that the nature of active Pd species for the combustion of methane is PdO_x.

2. Experimental

2.1. Preparation of catalysts

$LaFeO_3$ with perovskite-type structure was prepared by the amorphous citrate method [30,31]. Briefly, citric acid and metal nitrate solution (1:1 molar ratio) was subjected to complexation (at 60 °C for 1 h) followed by vacuum drying (at 70 °C for 2 h). The obtained orange spongy material was calcined at 700 °C for 2 h. The $Ce_xZr_{1-x}O_2$ (hereafter $CeZrO_2$) was calcined at 500 °C for 2 h. The supports $LaFeO_3$ and $CeZrO_2$ were impregnated with Pd from $Pd(NO_3)_2{\cdot}2H_2O$ solution. The as-prepared catalysts were dried at 110 °C for 10 h and subsequently calcined at 550 °C for 5 h. The composition and textural properties of the catalysts are presented in Table 1.

2.2. Characterization techniques

Inductively coupled plasma optical emission spectroscopy (ICP-OES): Palladium metal content in the catalysts was determined using an Agilent 7500cx ICP-OES analyzer. 10 mg catalyst was dissolved in 10 ml aqua regia in an ultrasonic bath. The resulting solution was made up to 50 ml with deionised (18 mΩ cm) water. The Pd content was determined as an average of three values.

Brunauer–Emmett–Teller (BET) surface area: Nitrogen adsorption and desorption isotherms at −196 °C were obtained on a BELSORP-max (BEL, Japan) instrument. Prior to the experiments, the samples were evacuated at 200 °C for 4 h. The total surface area of the samples was determined by the BET method.

X-ray diffraction (XRD): The powder XRD patterns of the catalysts were collected on a X'Pert Pro diffractometer (PANalytical) using the CuKα radiation (λ = 1.5148 Å, 35 kV and 40 mA) in the 2θ range of 20–80°. A step size of 0.020° and a step time of 2.5 s were used.

Temperature programmed reduction (TPR): H_2-TPR measurements were performed on a Quantachrome CHEMBET-3000 instrument to study the reducibility of PdO_x species supported on $CeZrO_2$ and $LaFeO_3$. The quartz reactor was loaded with 100 mg of catalyst and a K-type thermocouple was inserted into the middle of the catalyst bed to measure temperature. The samples were pre-treated in N_2 flow (25 ml min^{-1}) at 200 °C for 1 h followed by cooling down to −25 °C. Then H_2-TPR experiments were performed by introducing 5 vol.% H_2 in N_2 (25 ml min^{-1}) with a temperature ramp of 5 °C min^{-1} up to 850 °C. The H_2 uptake during the reduction process was measured with thermal conductivity detector (TCD) and the H_2O formed during the reduction was prevented from passing through the detector by adsorption onto a molecular sieve.

Visible Raman spectroscopy: Raman spectra were measured on a Renishaw 2000 spectrometer equipped with holographic notch filters for elastic scattering and a CCD array detector. WiRE software was used to collect the data. The samples were excited with the red laser (632.816 nm). The laser was focused onto the sample using the 50× objective that is mounted to the microscope. The instrument was calibrated with Si single crystal (Raman band at ≈520 cm^{-1}). The spectra were recorded at room temperature with an exposure time of 10 s and accumulation number of 60.

CO chemisorption: CO chemisorption measurements were performed on Micromeritics ASAP2010 instrument to assess the dispersion of Pd in the catalysts. Prior to CO chemisorption, catalysts were pre-treated at 300 °C for 1 h each in pure O_2 and in H_2 followed by evacuation at the same temperature for 30 min. Subsequently, the catalysts were cooled to room temperature by flowing pure He where CO chemisorption experiments were performed. Reversible isotherms were measured with an interim 30 min evacuation between isotherms. The amount of adsorbed CO was determined from the difference between these two isotherms. From this the dispersion was determined by assuming an adsorption stoichiometry of unity of CO and Pd. Hemispherical particle sizes were determined according to the procedure reported in [32].

CO adsorbed diffuse reflectance infrared Fourier transform spectroscopy (CO-DRIFTS): CO-DRIFTS experiments were conducted using a VERTEX 70 FT-IR spectrometer (Bruker Optics) equipped with a diffuse reflectance accessory (Praying Mantis, Harrick). The IR cell is equipped with CaF_2 windows and connected to a temperature programmer and gas-feeding system with mass-flow controllers. The catalysts (ca. 80 mg each) were pre-treated in He

Table 1
Chemical composition and physico-chemical properties of the catalysts.

Catalyst	Pd[a] (wt.%)	V^b_{total} ($cm^3\,g^{-1}$)	S_{BET}[c] ($m^2\,g^{-1}$)	Surface coverage[d] ($\mu mol\,CO\,g^{-1}_{cat}$)	Pd dispersion (%)	Pd particle size[d] (nm)
$CeZrO_2$	–	0.3	78	–	–	–
$Pd/CeZrO_2$	2.2	0.27	67	160.7	85.5	1.3
$LaFeO_3$	–	–	14	–	–	–
$Pd/LaFeO_3$	1.99	–	12	47.9	26	4.3

[a] ICP-OES.
[b] *t*-Plot method.
[c] BET method.
[d] Determined by a method reported in [32].

flow (50 ml min^{-1}) to 120 °C for 1 h followed by reduction in 10 vol.% H_2 in He flow (50 ml min^{-1}) at 300 °C for 1 h. Subsequently, the flow was switched to pure He (50 ml min^{-1}) for 30 min followed by cooling to room temperature. At this temperature, CO (5 vol.% CO in He at 50 ml min^{-1}) adsorption was carried out for 30 min followed by flushing with pure He for another 30 min. Difference spectra were recorded at room temperature by co-adding 200 scans at a resolution of 4 cm^{-1}.

X-ray absorption spectroscopy (XAS): XAS data were collected in transmission mode at the superXAS, Swiss Light Source (SLS), Villigen. Spectra were obtained at the Pd K-edge (24.3 keV). Ion chamber detectors were used to determine intensities of the incident (I_o) and transmitted (I_t) X-rays. Extended X-ray absorption fine structure (EXAFS) spectra were recorded on calcined catalysts at room temperature. *In situ* X-ray absorption near edge structure (XANES) spectra were recorded between ca. 250 and 750 °C during the combustion of methane to study the behaviour of Pd. To this end, the same micro-reactor setup that is well documented in [19,33] was employed. Briefly, the setup comprises of quartz capillary micro-reactor equipped with an air blower (serving as an oven), temperature programmer and a gas-feeding system with mass-flow controllers (Brooks). The capillary micro-reactor (1.0 mm diameter and ca. 6 cm length) was loaded with ca. 20 mg of catalyst, firmly packed between two plugs of quartz wool and fixed on to the oven. Prior to the combustion experiments, the catalysts were oxidatively pre-treated in 20 vol.% O_2 in He at a total flow of 50 ml min^{-1} at 300 °C for 30 min followed by cooling to ca. 250 °C. The behaviour of Pd species during the combustion of methane is monitored by changing the flow from O_2 to reaction mixture (1 vol.% CH_4 and 4 vol.% O_2 in He at a total flow of 50 ml min^{-1}) followed by ramping (5 °C min^{-1}) up to ca. 740 °C and cooling down to 250 °C. XANES spectra were recorded during the reaction. The *WINXAS* v3.1 software was used for XAS analysis [34]. The XAS data were energy calibrated, background subtracted and normalized. Pd metal foil and PdO were used as model compounds.

2.3. Combustion of methane

Activity tests were performed in a quartz tubular reactor of 6 mm internal diameter and 40 cm length. The reactor was loaded with catalyst (100 mg and sieve fraction of 150–200 μm) which was diluted with quartz particles of the same size in 1:1 volume ratio and firmly packed between two plugs of quartz wool. Then the reactor was positioned vertically in a programmable tube furnace. A thermocouple was inserted into the catalyst bed to measure the temperature. Prior to the combustion experiments, the catalysts were oxidatively pre-treated (20 vol.% O_2 in He at 100 ml min^{-1}) at 500 °C for 1 h followed by cooling to ca. 100 °C. At this temperature, the reaction mixture (1 vol.% CH_4 and 4 vol.% O_2 in He at a total flow of 100 ml min^{-1}) was introduced by a gas-feeding system comprising mass-flow controllers (Bronkhorst). The reaction was carried out between ca. 200 and 850 °C by switching the temperature ramp to the maximum temperature followed by cooling down to the initial temperature (programmed and controlled with controltherm software, Nabertherm). The gas hourly space velocity (GHSV) was 7000 h^{-1}. The reactor outlet was connected to a gas chromatograph (3000A microGC, Agilent Technologies) to analyze reaction products. The microGC was controlled with EZChrom Elite software.

3. Results and discussion

3.1. XRD

To study the support structure and Pd distribution in the catalysts XRD measurements were performed on pristine supports ($CeZrO_2$ and $LaFeO_3$) and catalysts (Pd/$CeZrO_2$ and Pd/$LaFeO_3$). The XRD patterns (not shown) of the catalysts were identical to those of the respective supports and showed no reflections attributable to either PdO or metallic Pd. This indicates that the dispersion of Pd was high and that the structure of the support was essentially the same in the catalysts even after Pd loading followed by pretreatments. The observations are consistent with earlier results reported on Pd/$CeZrO_2$ and Pd/$LaFeO_3$ [9,13,35]. Given the detection limit of XRD, the catalysts were analyzed by Raman spectroscopy to obtain information on the distribution of Pd in the catalysts.

3.2. Raman

Raman spectra of the pristine supports and catalysts are compared in Fig. 1. Pristine $CeZrO_2$ exhibits characteristic Raman bands of the $CeZrO_2$ phase (tetragonal t'') at 463 and 614 cm^{-1} [36]. A Raman band at 542 cm^{-1} could be due to the $CeZrO_2$ phase [36] or defects arising either from vacancies or from impurities [37]. By comparison, it can be seen from the Pd/$CeZrO_2$ spectrum that the intensity of the band at 465 cm^{-1} decreased drastically and a new prominent band at 649 cm^{-1} appeared. The latter is attributed to the B_{1g} Raman mode of PdO_x species [38]. The shape and intensity of the band imply that PdO_x species are highly dispersed in the catalyst and thus could not be detected by XRD.

The support $LaFeO_3$ shows two Raman bands at 431 and 650 cm^{-1} which are frequently observed for this perovskite-type structure [39–42]. The band at 431 cm^{-1} was previously assigned to the B_{3g} mode due to one phonon scattering. On the other hand, the assignment of the band at 650 cm^{-1} is not straightforward [43–45], it could be due to two phonon or impurity scattering [40]. These two Raman bands can still be seen in the spectrum of Pd/$LaFeO_3$ however, the band at 650 cm^{-1} is now centered at 615 cm^{-1}, grown in intensity and broadened (between 500 and 715 cm^{-1}). Previously, the B_{1g} vibrational mode of PdO_x species on Pd/Al_2O_3 was observed at 625 cm^{-1}. Taking this into account, it can be suggested that the band at 615 cm^{-1} is a combination of two bands that are arising from PdO_x species and from the perovskite crystal structure leaving a certain degree of uncertainty on the dispersion of Pd in the catalyst. Therefore, the catalysts were further analyzed by EXAFS spectroscopy which is known to provide information even on the short range order.

3.3. EXAFS

The local microstructure of Pd species in the catalysts is studied by the k^3-weighted Fourier transform (FT) of EXAFS functions, non-

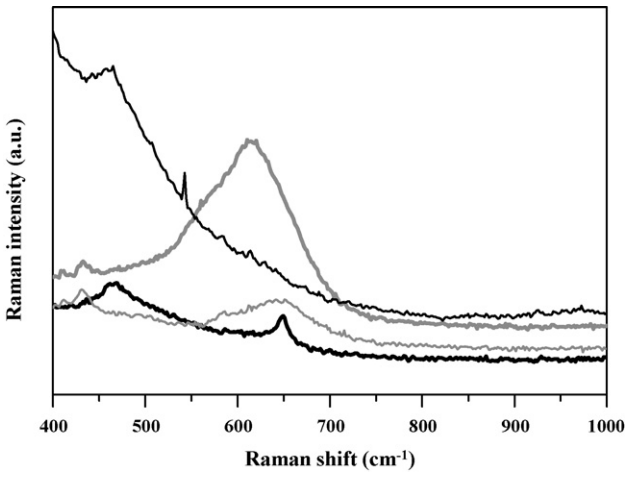

Fig. 1. Visible Raman spectra (taken at room temperature) of $CeZrO_2$ (black thin), Pd/$CeZrO_2$ (black thick), $LaFeO_3$ (gray thin) and Pd/$LaFeO_3$ (gray thick).

phase shift corrected. The EXAFS spectra of $Pd/CeZrO_2$ and $Pd/LaFeO_3$ are compared with the reference spectra of Pd metal foil and PdO in Fig. 2. The Pd metal foil reference spectrum shows a prominent peak at 2.45 Å. Such a peak was frequently observed for bulk Pd metal and can be attributed to Pd–Pd in the first coordination shell [19,46,47]. The bulk PdO reference sample exhibits two prominent peaks at 1.5 and 3 Å which can be attributed to Pd–O (first coordination shell) and Pd–Pd (second coordination shell) bond distances, respectively [19,46,47]. In addition, the latter peak contains a shoulder at 2.35 Å suggesting that the bulk PdO reference sample also contains a fraction of PdO_x species with shorter Pd–Pd bond distances. It is evident from the reference sample spectra that the intensity of the prominent peak is higher for bulk metallic Pd than the bulk PdO indicating a higher coordination number in the former than in the latter [46,47].

Against this background, it can be readily seen that $Pd/CeZrO_2$ and $Pd/LaFeO_3$ exhibit, in general, a main peak at around 1.5 Å attributable to the backscattering from oxygen neighbours in the first coordination shell which is also prominent in the spectrum of bulk PdO reference sample. This implies that Pd is completely in oxidized state in the catalysts after calcination. By strictly comparing the spectra of $Pd/CeZrO_2$ and $Pd/LaFeO_3$ it is evident that the Pd–O bond distance is shorter in the former (1.46 Å) than that in the latter (1.52 Å). This suggests that the PdO_x species are smaller in $Pd/CeZrO_2$ than in $Pd/LaFeO_3$. Significantly, peaks in the higher coordination shells are very weak in the spectra of the catalysts unlike in the bulk PdO reference spectrum suggesting a greater disorder in PdO_x species which in turn implies that they are very small in size. These observations indicate that Pd is highly dispersed in the catalysts which is in good agreement with XRD and Raman results as well as with the literature [9,13,35]. The results are further corroborated by other physico-chemical techniques that are more sensitive to highly dispersed Pd in the catalysts as discussed below.

3.4. H_2-TPR

TPR profiles of the two catalysts ($Pd/CeZrO_2$ and $Pd/LaFeO_3$) and the corresponding pristine supports are presented in Fig. 3. The reduction of pristine support $CeZrO_2$ occurs slowly and in two steps as seen by a narrow hydrogen uptake peak at 363 °C and a broad peak at 540 °C which is characteristic for Ce oxide. The former peak can be attributed to the reduction of surface CeO_2 and the latter to the reduction of bulk CeO_2, respectively [35,48]. The

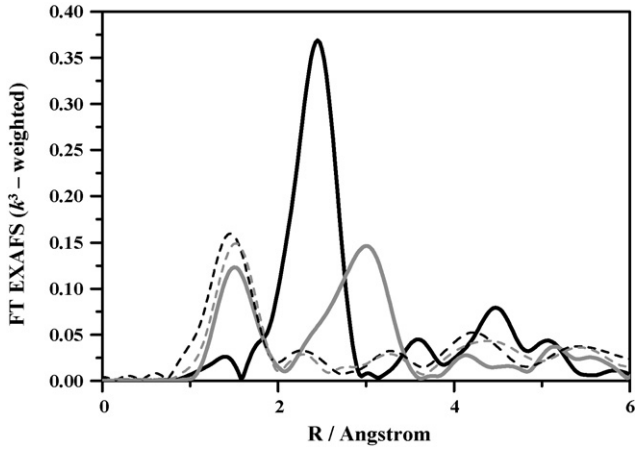

Fig. 2. Ex situ EXAFS (k^3-weighted, phase uncorrected and Fourier transformed) of the model compounds and the catalysts: bulk metallic Pd (black thick full line), bulk PdO (gray thick full line), $Pd/CeZrO_2$ (black thin broken line) and $Pd/LaFeO_3$ (gray thin broken line).

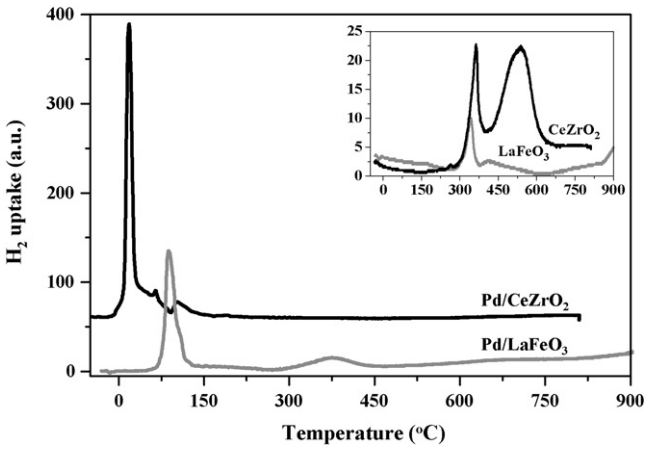

Fig. 3. Hydrogen TPR profiles of the pristine supports (inset) and catalysts.

reduction of pristine support $LaFeO_3$ also proceeds slowly as evidenced by a peak at 342 °C. Such a TPR peak was often observed on different Fe containing materials [49–51]. A TPR peak at 317 °C observed on $LaFeO_3$, which is relevant to the present study, was ascribed by the authors [49] to the reduction of a fraction of $Fe^{4+} \rightarrow Fe^{3+}$ within the perovskite structure. On the other hand, such a peak was also attributed to the reduction of extra-frame work $Fe^{3+}O_x \rightarrow Fe^{2+}O_x$ species in Fe-ZSM-5 [50]. Therefore, the TPR peak we observed for pristine $LaFeO_3$ could be due to the contribution from the reduction of $Fe^{4+}O_x$ and $Fe^{3+}O_x$ species occurring within the perovskite and on the surface, respectively.

In contrast, the reduction of $Pd/CeZrO_2$ and $Pd/LaFeO_3$ proceeds very rapidly as evidenced by the corresponding hydrogen uptake peaks in Fig. 3. The intensity of the peaks is much higher than that observed for the pristine supports indicating the reduction of PdO_x species in the catalysts. $Pd/CeZrO_2$ exhibits a narrow intense peak at 19 °C which contains a weak shoulder at 66 °C and a weak peak at 106 °C. By comparison, a previous study on 2 wt.% Pd on $CeZrO_2$ showed two peaks at 60 and 170 °C. These two peaks were assigned to the reduction of PdO and $CeZrO_2$, respectively [28]. Differently, the reduction of PdO in Pd/Ce-Zr and Pd/Ce-Zr-La was proposed to occur in two steps at 100 and 150 °C [52]. However when the same amount of Pd was supported on the $Ce\text{-}ZrO_2/Al_2O_3$, it exhibits TPR peaks at 12, 40 and around 120 °C [29]. Because the former two peaks are similar to that observed on Pd/Al_2O_3, the authors assigned these three peaks to the reduction of highly dispersed PdO species on alumina-rich grains, Ce-Zr-rich grains and more stable PdO species, respectively [29]. Based on this, we assign the peak at 19 °C observed for $Pd/CeZrO_2$ to the reduction of highly dispersed PdO_x species. This suggests that the support $CeZrO_2$ favours higher dispersion of Pd which is different from previous reports [28,29,52]. The TPR peak at 66 °C observed as a shoulder to the main peak at 19 °C could be due to the reduction of relatively stable PdO_x species. The weak peak at 106 °C could be due to the reduction of relatively more stable PdO_x species or of CeO_2 via the well known spillover mechanism [28]. For $Pd/LaFeO_3$, the hydrogen uptake peaks are shifted to higher temperatures as compared to $Pd/CeZrO_2$ indicating that the dispersion of Pd is not as high as in the latter. $Pd/LaFeO_3$ exhibits a main peak at 88 °C that contains a shoulder at 110 °C and a broad high temperature peak at 380 °C. The former two peaks are ascribed to the reduction of PdO_x species and the latter is similar to that observed for pristine $LaFeO_3$ (see above and Fig. 3). By comparing $Pd/CeZrO_2$ and $Pd/LaFeO_3$ it is evident that the dispersion of Pd is higher in the former than that in the latter which is in line with the EXAFS results. The surface morphology of PdO_x species in the catalysts was further

investigated by CO adsorbed DRIFTS to gain information at the atomic level.

3.5. CO-DRIFTS

CO adsorption is a widely used tool to investigate the morphology of Pd surface, thereby the degree of dispersion, by probing the vibrational mode of CO which is sensitive to the adsorption site on the Pd and thus on what extent the molecule is perturbed [53]. Therefore, $Pd/CeZrO_2$ and $Pd/LaFeO_3$ were analyzed by CO-DRIFTS to complement TPR data and to obtain a more clear picture on the distribution of Pd species in the catalysts. Background subtracted DRIFTS spectra of the catalysts after adsorption of CO followed by flushing with He for 30 min are shown in Fig. 4. Striking differences in adsorbed CO stretching bands between the two spectra of $Pd/CeZrO_2$ and $Pd/LaFeO_3$ can be seen. This infers that some adsorption sites available for CO are not the same in the catalysts [32]. The spectrum of $Pd/CeZrO_2$ exhibits two well defined bands at 2083 (intense) and 2141 (weak) cm^{-1} and virtually no bands between 2000 and 1900 cm^{-1}. The bands at 2083 and 2141 cm^{-1} are often attributed to CO adsorbed linearly on Pd^0 (Pd^0-CO) and Pd^{2+} (Pd^{2+}-CO), respectively [32,53,54]. These observations infer that the dispersion of Pd is high and homogeneous in $Pd/CeZrO_2$ and that not more than two kinds of Pd species exist in the catalyst which is profoundly consistent with the TPR results.

In contrast to the spectrum of $Pd/CeZrO_2$, $Pd/LaFeO_3$ shows a variety of carbonyl stretching bands indicating the presence of a number of different Pd sites in the catalyst. The spectrum is dominating with the low frequency bands at 1962, 1949 and 1896 cm^{-1} besides the 2082 cm^{-1} band which contains a shoulder at 2073 cm^{-1}. Based on the literature, the band at 1962 cm^{-1} may be ascribed to the μ_2 bridge bonded CO on Pd(1 0 0) facets, particle edges and steps. The feature at 1949 cm^{-1} could also be due to the μ_2 bridging of CO to Pd perhaps at the edges. The band at 1896 cm^{-1} is attributable to μ_3 bonded CO on Pd(1 1 1) or μ_2 bonded CO on Pd(1 0 0) planes. All these bands unambiguously confirm that the dispersion of Pd is relatively heterogeneous, consistent with TPR results [32,53,54].

H_2-TPR and CO-DRIFTS results show that the mean Pd particle size is smaller in $Pd/CeZrO_2$ than that in $Pd/LaFeO_3$. This is further confirmed by CO chemisorption. The mean Pd particle size in the catalysts is calculated assuming a spherical particle shape (Table 1). It determines that the mean Pd particle size is 1.3 and 4.3 nm for $Pd/CeZrO_2$ and $Pd/LaFeO_3$, respectively. Given the different size of Pd particles in the catalysts, the degree of coordination unsaturation of Pd atoms in the particles is likely to be different. Consequently, the surface of smaller Pd particles in $Pd/CeZrO_2$ could mostly be terminated by corners while in relatively larger particles in $Pd/LaFeO_3$ the surface is composed of not only corners but also edges and Pd(1 1 1) planes. It means that the proportion of corner sites decreases with increasing size of Pd particles from 1.3 to 4.3 nm which is in excellent agreement with CO-DRIFTS observations. CO adsorbed DRIFTS spectrum of $Pd/CeZrO_2$ exhibits a narrow band at 2083 cm^{-1} reflecting the linear adsorption of CO merely to corners sites. In marked contrast, $Pd/LaFeO_3$ shows low frequency stretching bands (2000–1800 cm^{-1}) besides a broad high frequency band at 2083 cm^{-1} confirming that the surface of Pd particles in the catalyst is composed of multiple adsorption sites.

3.6. Combustion of methane

Combustion of methane on $Pd/CeZrO_2$ and $Pd/LaFeO_3$ was performed over a wide temperature range to study the combustion performance of the catalysts (Fig. 5). On $Pd/CeZrO_2$, considerable combustion activity was already observed at 250 °C and complete methane conversion was observed at around 380 °C. Interestingly, the conversion was 100% even up to 800 °C which is not typical for Pd-based catalysts reported (see e.g. [12,13,19]). However, while cooling from 800 °C a loss in the methane conversion was observed between 680 and 560 °C with a maximum loss of only 1% at around 600 °C leaving a typical hysteresis in the reaction rate (see the inset in Fig. 5). After that, the catalyst again attains a 100% conversion between 560 and 350 °C and, below this temperature the methane conversion gradually decreased. Interestingly, the catalyst is more active while cooling from 800 to 150 °C than while heating-up. In general, this can be attributed to the altered Pd dispersion in $Pd/CeZrO_2$. Plausibly, the dispersion of Pd might have decreased in the catalyst during the first run (i.e., heating) thus the improved catalytic performance in the second run (i.e., cooling) [22]. This can be correlated with previous reports which conclude that the combustion of methane is "structure sensitive" and that relatively larger Pd particles are more active than the smaller ones [18,22,55,56], though there is no consensus [57]. However, the improved catalytic performance of $Pd/CeZrO_2$ is superior than on previously reported catalysts, for example on 4 wt.% Pd/Al_2O_3 which is also one of the TWC components [17]. Also, the loss in the reaction rate observed during hysteresis is much smaller on $Pd/CeZrO_2$ than on other catalysts reported [17,19,58]. For instance, combustion activity on Pd/ZrO_2 (10 wt.% Pd) decreased while cooling with a maximum loss in the reaction rate of almost two

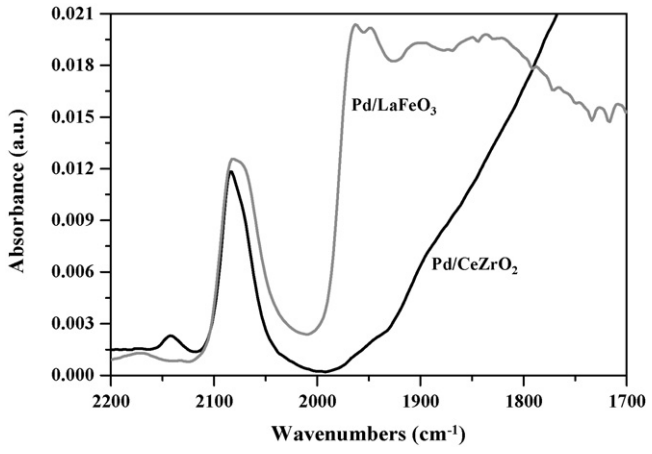

Fig. 4. DRIFT spectra of CO adsorbed on the reduced catalysts.

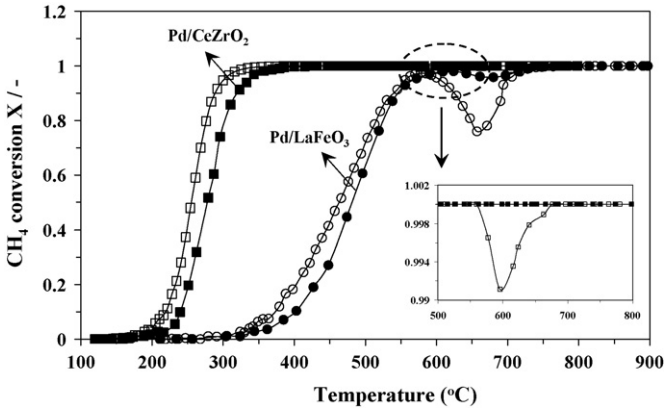

Fig. 5. Conversion of methane profiles over the catalysts: Heating (filled symbols) and Cooling (open symbols). For the sake of visibility, the conversion profiles between 500 and 800 °C over $Pd/CeZrO_2$ are shown in the inset. Reaction conditions as described in Section 2.3.

orders of magnitude higher than on $Pd/CeZrO_2$ [19]. These observations demonstrate that $Pd/CeZrO_2$ exhibits the best activity and stability compared to any other catalysts reported so far, to the best of our knowledge [12,13,17,19,55,58,59], for the combustion of methane in a wide temperature range typically encountered in practical applications.

The combustion of methane profiles on $Pd/LaFeO_3$ during heating and cooling are also presented in Fig. 5. From the conversion profiles it is evident that $Pd/LaFeO_3$ is less active than $Pd/CeZrO_2$. Considerable methane conversion was only detected above 400 °C and the complete conversion was observed above 750 °C. Interestingly, the typical hysteresis loop due to loss in the reaction rate was observed in both the runs between 580 and 740 °C which is different from that on $Pd/CeZrO_2$ on which the hysteresis was observed only while cooling. Nevertheless on $Pd/LaFeO_3$, the loss in the methane conversion is more significant (ca. 24%) while cooling than while heating (ca. 5%). By comparison, the loss of methane conversion is more than an order of magnitude higher on $Pd/LaFeO_3$ than that on $Pd/CeZrO_2$ indicating that the latter is better for this reaction. Similar to $Pd/CeZrO_2$, $Pd/LaFeO_3$ also shows high activity while cooling (below 580 °C) but it never reached a 100% conversion unlike on the former. The increased activity could be due to altered dispersion of Pd in the catalyst as discussed above for $Pd/CeZrO_2$. Therefore, it is of interest to monitor the behaviour of Pd in both catalysts during the combustion of methane by XANES that is suitable technique even at high temperatures (>700 °C) and provides information on the oxidation state of Pd during the reaction.

3.7. In situ XANES

The behaviour of Pd in the catalysts was monitored by XANES aiming to analyze the catalytic performance of $Pd/CeZrO_2$ and $Pd/LaFeO_3$. To this end, temperature programmed combustion of methane was performed between ca. 250 and 730 °C during heating and cooling to the initial reaction temperature. XANES spectra were recorded during the reaction and the corresponding spectra are depicted in Fig. 6. For each catalyst four spectra are shown to assess the state of Pd at different stages of the reaction and the spectra correspond to the combustion profiles on both the catalysts described in Section 3.6 and Fig. 5. They are: (a) initial spectrum (i.e., after oxidative pre-treatment and before switching to reaction mixture), (b) at the maximum methane conversion while heating in the reaction mixture, (c) at the maximum loss of methane conversion observed in the hysteresis (i.e., while cooling), and (d) again after attaining a maximum conversion.

Starting with $Pd/CeZrO_2$, the initial spectrum (black full line) is characteristic for PdO in which Pd is in 2+ oxidation state. During the temperature programmed reaction the spectrum does virtually not change as observed in a spectrum taken at 586 °C (see light gray spectrum) at which complete combustion of methane was recorded in the catalytic tests (see inset, Fig. 5). This indicates that the oxidation state of Pd is essentially 2+ when the combustion performance of the catalyst is at the best pointing to the important role of PdO_x species in the reaction. Even at 700 °C the spectrum (black broken line) is essentially the same as the initial spectrum (full line) suggesting that the state of Pd in $Pd/CeZrO_2$ is PdO_x during the reaction up to this temperature. Having performed the reaction up to 730 °C, the reactor was cooled down to the initial temperature. During this, a significant change in the intensity of the edge and its position was observed in the spectrum taken at 635 °C. The intensity of the edge decreased slightly and its position red shifted implying that at this temperature a fraction of PdO_x is reduced in which the oxidation state of Pd is lower than 2+. It is noteworthy that the hysteresis during activity test (depicted in Fig. 5 inset) was observed between 700 and 550 °C and a maximum loss in the methane conversion was at around 600 °C. Therefore, the hysteresis can be attributed to the reduction (or decomposition) of PdO_x which is indeed in line with the previous studies reported on Pd/Al_2O_3 and Pd/ZrO_2 [17,19]. The difference between the present and previously reported catalysts may lie in the extent of PdO decomposition. Given the nature of the support

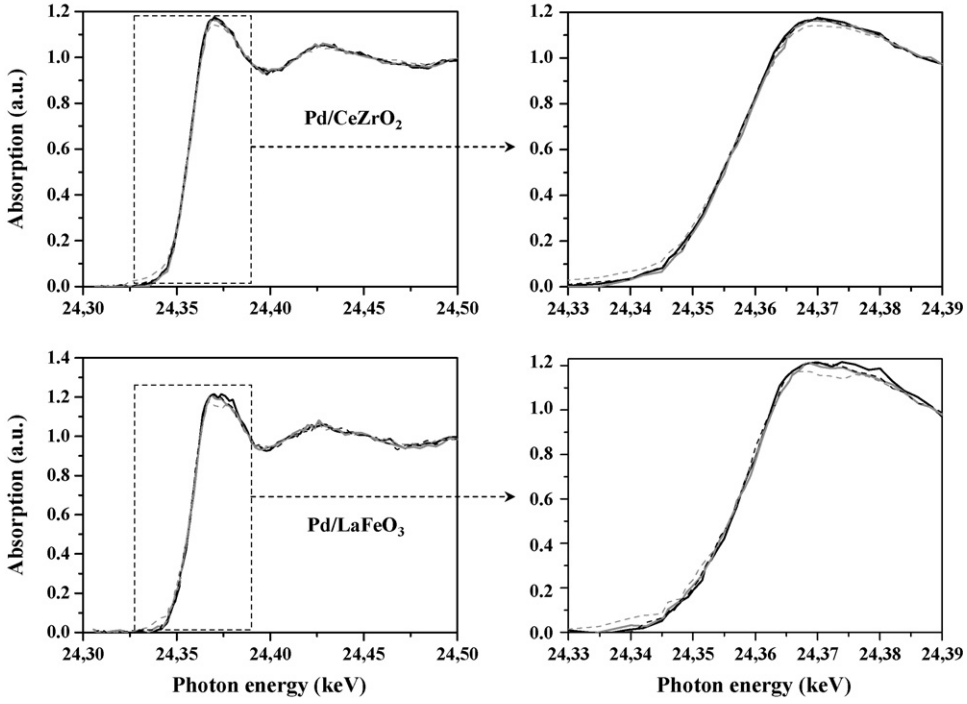

Fig. 6. In situ XANES of the catalysts taken during the temperature programmed reaction: initial spectrum after oxidative pre-treatment (black full line: at 250 °C ($Pd/CeZrO_2$) or 314 °C ($Pd/LaFeO_3$), at a maximum methane conversion while heating (gray full line: at 586 °C ($Pd/CeZrO_2$) or 661 °C ($Pd/LaFeO_3$), at ca. 730 °C (black broken line) and at 635 °C ($Pd/CeZrO_2$) or 650 °C ($Pd/LaFeO_3$) where the hysteresis was observed (Fig. 5) while cooling (gray broken line). Reaction conditions as described in Section 2.2.

$CeZrO_2$, the decomposition of PdO_x in $Pd/CeZrO_2$ may have virtually been prevented as evidenced by a loss of only 1% methane conversion (Fig. 5) as compared to ca. 100% on Pd/ZrO_2, for example. In agreement with the catalytic results, below 550 °C the spectrum was restored to the initial state (not shown for the sake of clarity) at which complete conversion of methane was observed (Fig. 5). This confirms that the nature of active Pd species in $Pd/CeZrO_2$ for the combustion of methane, temperatures up to 700 °C, is PdO_x in which Pd is in 2+ oxidation state.

In situ XANES spectra of $Pd/LaFeO_3$ are also presented in Fig. 6. Similar spectral changes can be seen as observed for $Pd/CeZrO_2$ however, at different temperatures that correspond well with the combustion profiles presented in Fig. 5. After oxidative pre-treatment (initial spectrum, black full line), the spectrum represents the reference PdO suggesting that the typical oxidation state of Pd in the catalyst is 2+. From the catalytic results it is evident that the conversion of methane drops between 580 and 740 °C with a maximum drop of 5% at 660 °C during the first run. From the corresponding spectrum at 661 °C it is evident that a small fraction of PdO_x is reduced in the catalyst as seen by a slight decrease in the intensity of the white line and a little red shift in the position of the edge. In comparison, the spectrum (black broken line) taken at 734 °C (the maximum temperature could be reached with our setup) is slightly reoxidized. In agreement with this, the conversion of methane is considerably recovered at this temperature but complete conversion occurred only above 750 °C (see Fig. 3). As expected, while cooling from 734 °C a dramatic decrease in the intensity of the edge that is accompanied by a well known red shift in the edge position was observed at 650 °C (see gray broken line spectrum). The temperature coincides well with that at which hysteresis was observed in the conversion profile with a maximum loss of 24% in the conversion of methane at 650 °C. These observations corroborate well with our above conclusion that the nature of active sites for the combustion of methane is PdO_x.

By comparing the in situ XANES spectra of $Pd/LaFeO_3$ and $Pd/CeZrO_2$ taken around 650 °C, at which a maximum loss in the conversion was observed during cooling (Fig. 5), it is evident that the observed spectral changes are more pronounced for the former than for the latter. This suggests that the reduction of PdO_x is more pronounced in $Pd/LaFeO_3$ than that in $Pd/CeZrO_2$ which can be attributed to the nature of the supports and the PdO_x domain size [60]. It implies that the support $LaFeO_3$ perovskite is not as effective as $CeZrO_2$ in preventing PdO_x from releasing oxygen (i.e., from decomposition) which complies with the oxygen storage capacity (OSC) of the supports [61–64]. From the literature it is evident that the extent of loss of activity during the hysteresis is dependent on the nature of the catalyst, $CeZrO_2$ based catalysts being better than the other [12,13,24,58–60]. From in situ XANES observations together with the catalytic data, it can be suggested that $Pd/CeZrO_2$ can be more effective for the combustion of methane under lean conditions than $Pd/LaFeO_3$ even at high temperature fluctuations that are often encountered in automobile operations.

4. Conclusions

The combustion of methane with model three way catalysts was studied in the temperature range between ca. 200 and 850 °C with the aim to evaluate the behaviour of Pd at high temperatures under lean conditions. To this end, $Pd/CeZrO_2$ and $Pd/LaFeO_3$ were prepared by incipient wetness impregnation and the nature and distribution of Pd species in the catalysts was analyzed by a variety of physico-chemical techniques. The behaviour of Pd in the catalysts during the reaction was monitored by in situ XANES. On the basis of these results, the following main conclusions can be drawn:

- The dispersion of Pd is higher in the catalyst $Pd/CeZrO_2$ than in $Pd/LaFeO_3$ perovskite.
- $Pd/CeZrO_2$ is more active and stable than $Pd/LaFeO_3$ for the combustion of methane in a wide temperature range. The loss in methane conversion observed in the hysteresis is negligible (1%) on the former, while it is significant (24%) on the latter after subjecting the catalysts to high temperatures.
- In situ XANES revealed that Pd is in highly oxidized state when the catalysts were performing the combustion reaction at their best and that Pd is slightly reduced during the hysteresis, however to different extents in the two catalysts. The active Pd species for the combustion of methane are PdO_x.

Acknowledgements

The authors are grateful to Empa for financial support. The authors also thank the team at the SuperXAS, Swiss Light Source (SLS) at the PSI Villigen, Switzerland for their help during the XAS experimental campaign.

References

[1] J. Pérez-Ramírez, Appl. Catal. B 70 (2007) 31.
[2] B.C.H. Steele, Nature 400 (1999) 619.
[3] J.K. Lampert, M.S. Kazi, R.J. Farrauto, Appl. Catal. B 14 (1997) 211.
[4] R.J. Farrauto, R.M. Heck, Catal. Today 51 (1999) 351.
[5] C. Bozo, N. Guilhaume, J.M. Herrmann, J. Catal. 203 (2001) 393.
[6] F. Klingstedt, A.K. Neyestanaki, R. Byggningsbacka, L.E. Lindfors, M. Lunden, M. Petersson, P. Tengstrom, T. Ollonqvist, J. Vayrynen, Appl. Catal. A 209 (2001) 301.
[7] C. Pliangos, I.V. Yentekakis, V.G. Papadakis, C.G. Vayenas, X.E. Verykios, Appl. Catal. B 14 (1997) 161.
[8] Y. Nishihata, J. Mizuki, T. Akao, H. Tanaka, M. Uenishi, M. Kimura, T. Okamoto, N. Hamada, Nature 418 (2002) 164.
[9] M. Uenishi, M. Taniguchi, H. Tanaka, M. Kimura, Y. Nishihata, J. Mizuki, T. Kobayashi, Appl. Catal. B 57 (2005) 267.
[10] H. Tanaka, M. Uenishi, M. Taniguchi, I. Tan, K. Narita, M. Kimura, K. Kaneko, Y. Nishihata, J. Mizuki, Catal. Today 117 (2006) 321.
[11] B.M. Reddy, P. Lakshmanan, P. Bharali, P. Saikia, G. Thrimurthulu, M. Muhler, W. Grünert, J. Phys. Chem. C 111 (2007) 10478.
[12] E. Tzimpilis, N. Moschoudis, M. Stoukides, P. Bekiaroglou, Appl. Catal. B 84 (2008) 607.
[13] S. Specchia, E. Finocchio, G. Busca, G. Saracco, V. Specchia, Catal. Today 143 (2009) 86.
[14] S. Furfori, N. Russo, D. Fino, G. Saracco, V. Specchia, Chem. Eng. Sci. 65 (2010) 120.
[15] A. Winkler, P. Dimopoulos, R. Hauert, C. Bach, M. Aguirre, Appl. Catal. B 84 (2008) 162.
[16] A. Winkler, D. Ferri, R. Hauert, Catal. Today, (2009) doi:10.1016/j.cattod.2008.11.021.
[17] R.J. Farrauto, M.C. Hobson, T. Kennelly, E.M. Waterman, Appl. Catal. A 81 (1992) 227.
[18] C.A. Muller, M. Maciejewski, R.A. Koeppel, A. Baiker, J. Catal. 166 (1997) 36.
[19] J.-D. Grunwaldt, N. van Vegten, A. Baiker, Chem. Commun. (2007) 4635.
[20] M. Lyubovsky, L. Pfefferle, Catal. Today 47 (1999) 29.
[21] J.N. Carstens, S.C. Su, A.T. Bell, J. Catal. 176 (1998) 136.
[22] O. Demoulin, G. Rupprechter, I. Seunier, B. Le Clef, M. Navez, P. Ruiz, J. Phys. Chem. B 109 (2005) 20454.
[23] S. Guerrero, P. Araya, E.E. Wolf, Appl. Catal. A 298 (2006) 243.
[24] P. Forzatti, Catal. Today 83 (2003) 3.
[25] J.G. McCarty, Catal. Today 26 (1995) 283.
[26] R. Burch, F.J. Urbano, Appl. Catal. A 124 (1995) 121.
[27] S. Yang, A. Maroto-Valientea, M. Benito-Gonzaleza, I. Rodriguez-Ramosa, A. Guerrero-Ruiz, Appl. Catal. B 28 (2000) 223.
[28] M.F. Luo, X.M. Zheng, Appl. Catal. A 189 (1999) 15.
[29] R. Zhou, B. Zhao, B. Yue, Appl. Surf. Sci. 254 (2008) 4701.
[30] M.S.G. Baythoun, F.R. Sale, J. Mater. Sci. 17 (1982) 2757.
[31] E. Krupicka, A. Reller, A. Weidenkaff, Cryst. Eng. 5 (2002) 195.
[32] T. Lear, R. Marshall, J.A. Lopez-Sanchez, S.D. Jackson, T.M. Klapotke, M. Baumer, G. Rupprechter, H.J. Freund, D. Lennon, J. Chem. Phys. 123 (2005) 174706.
[33] J.-D. Grunwaldt, M. Caravati, S. Hannemann, A. Baiker, Phys. Chem. Chem. Phys. 6 (2004) 3037.
[34] T. Ressler, J. Synch. Rad. 5 (1998) 118.
[35] C. Larese, F.C. Galisteo, M.L. Granados, R. Mariscal, J.L.G. Fierro, M. Furio, R.F. Ruiz, Appl. Catal. B 40 (2003) 305.
[36] A. Iglesias-Juez, A. Martinez-Arias, M. Fernandez-Garcia, J. Catal. 221 (2004) 148.
[37] J.E. Spanier, R.D. Robinson, F. Zhang, S.W. Chan, I.P. Herman, Phys. Rev. B 64 (2001) 245407.
[38] J.R. McBride, K.C. Hass, W.H. Weber, Phys. Rev. B 44 (1991) 5016.
[39] Y. Wang, J. Zhu, L. Zhang, X. Yang, L. Lu, X. Wang, Mater. Lett. 60 (2006) 1767.
[40] M. Popa, J. Frantti, M. Kakihana, Solid State Ionics 154–155 (2002) 437.

[41] T. Asada, T. Kayama, H. Kusaba, H. Einaga, Y. Teraoka, Catal. Today 139 (2008) 37.
[42] M. Popa, J. Frantti, M. Kakihana, Solid State Ionics 154–155 (2002) 135.
[43] N. Koshizuka, S. Ushioda, Phys. Rev. B 22 (1980) 5394.
[44] S. Venugopalan, M. Dutta, A.K. Ramdas, J.P. Remeika, Phys. Rev. B 31 (1985) 1490.
[45] V.B. Podobedov, A. Weber, D.B. Romero, J.P. Rice, H.D. Drew, Phys. Rev. B 58 (1998) 43.
[46] G.L. Chiarello, J.-D. Grunwaldt, D. Ferri, F. Krumeich, C. Oliva, L. Forni, A. Baiker, J. Catal. 252 (2007) 127.
[47] D. Grandjean, R.E. Benfield, C. Nayral, A. Maisonnat, B. Chaudret, J. Phys. Chem. B 108 (2004) 8876.
[48] H.C. Yao, Y.F. Yu Yao, J. Catal. 86 (1984) 254.
[49] P. Porta, S. Cimino, S. De Rossi, M. Faticanti, G. Minelli, I. Pettiti, Mater. Chem. Phys. 71 (2001) 165.
[50] M. Schwidder, M. Santhosh Kumar, K. Klementiev, M.M. Pohl, A. Brückner, W. Grünert, J. Catal. 231 (2005) 314.
[51] F. Heinrich, C. Schmidt, E. Löffler, M. Menzel, W. Grünert, J. Catal. 212 (2002) 157.
[52] Y. Guo, G. Lu, Z. Zhigang, S. Zhang, Y. Qi, Y. Liu, Catal. Today 126 (2007) 296.
[53] W. Daniell, H. Landes, N.E. Fouad, H. Knözinger, J. Mol. Catal. A 178 (2002) 211.
[54] S. Bertarione, D. Scarano, A. Zecchina, V. Johanek, J. Hoffmann, S. Schauermann, M.M. Frank, J. Libuda, G. Rupprechter, H.J. Freund, J. Phys. Chem. B 108 (2004) 3603.
[55] T. Schalow, B. Brandt, D.E. Starr, M. Laurin, S.K. Shaikhutdinov, S. Schauermann, J. Libuda, H.-J. Freund, Angew. Chem. 118 (2006) 3775.
[56] K. Fujimoto, F.H. Ribeiro, M. Avalos-Borja, E. Iglesia, J. Catal. 179 (1998) 431.
[57] G. Zhu, J. Han, D.Y. Zemlyanov, F.H. Ribeiro, J. Am. Chem. Soc. 126 (2004) 9896.
[58] L.M.T. Simplicio, S.T. Brandao, D. Domingos, F. Bozon-Verduraz, E.A. Sales, Appl. Catal. A 360 (2009) 2.
[59] G. Groppi, C. Cristiani, L. Lietti, C. Ramella, M. Valentini, P. Forzatti, Catal. Today 50 (1999) 399.
[60] R.J. Farrauto, J.K. Lampert, M.C. Hobson, E.M. Waterman, Appl. Catal. B 6 (1995) 263.
[61] W.J. Stark, M. Maciejewski, L. Madler, S.E. Pratsinis, A. Baiker, J. Catal. 220 (2003) 35.
[62] M. Zhao, M. Shen, J. Wang, J. Catal. 248 (2007) 258.
[63] M. Uenishi, H. Tanaka, M. Taniguchi, I. Tan, Y. Sakamoto, S. Matsunaga, K. Yokota, T. Kobayashi, Appl. Catal. A 296 (2005) 114.
[64] S. Royer, H. Alamdari, D. Duprez, S. Kaliaguine, Appl. Catal. B 58 (2005) 273.